

# **Quantification of Modeling Uncertainties Based on the Blind Prediction Contest Submissions**

Siamak Sattar<sup>1</sup>, Abbie B. Liel<sup>1</sup>, Paolo Martinelli<sup>2</sup>

<sup>1</sup>Department of Civil, Environmental and Architectural Engineering, University of Colorado-Boulder, 1111 Engineering Drive, ECOT 440, 428 UBC, Boulder, CO, 80309; email: sattar@colorado.edu; abbie.liel@colorado.edu

<sup>2</sup>Department of Civil and Environmental Engineering, Politecnico di Milano, Piazza L. da Vinci 32, 20133, Milan, Italy; email: pmartinelli@mail.stru.polimi.it

## **ABSTRACT**

Modeling uncertainty can have a significant impact on the assessed risk of earthquake-induced damage and collapse in a building obtained through the performance-based earthquake engineering framework. This paper quantifies the effect of modeling uncertainty on performance-based risk assessments, accounting for differences in software platforms, solution algorithm, element-types, and model parameter calculation or selection, using results of the 7-story reinforced concrete (RC) building blind prediction contest (2006) at University of California at San Diego (UCSD). The blind prediction test data provide a unique opportunity to quantify the influence of modeling uncertainty on structural response predictions.

In this study, the bias and variability of predicted drift in the contest submissions are taken to represent modeling uncertainty. The modeling uncertainty quantified from the UCSD test submissions is combined with uncertainty due to record-to-record variability and a set of fragility curves are computed for different drift levels. The final fragility curves account for modeling and ground motion uncertainty. Results are compared with the results with no modeling uncertainty. The key contribution of this study is to investigate the uncertainty embedded in the response due to combination of ground motion and modeling uncertainty.

## **INTRODUCTION**

In the assessment of the seismic performance of a building, two main sources of uncertainty are present: (a) uncertainty due to the selected ground motions used in the analysis, known as record-to-record uncertainty, and (b) uncertainty embedded in the simulation model, known as modeling uncertainty. Quantification and propagation of these sources of uncertainty through the assessment of seismic risk is one of the important aspects of the performance-based earthquake engineering (PBEE) framework. Uncertainty due to record-to-record (RTR) variability stems from variation in the response of the structure excited by different ground motions due to the specific characteristics of each record, such as frequency content. RTR uncertainty is incorporated in the PBEE framework through the development of robust techniques for ground motion selection and scaling whereby multiple ground motions, selected to represent the seismicity at the site of interest, are used in the

assessment (Haselton et al. 2007). Modeling uncertainty stems from variation in the physical properties of the building components, as well as variation in the representation of these properties in an analysis model. Past research in the area of modeling uncertainty considered variation of different modeling parameters such as element strength, initial stiffness, hardening stiffness, plastic rotation capacity, and hysteretic energy dissipation capacity to quantify the significance of modeling uncertainty in seismic risk assessment (Ellingwood et al. 1980; Fardis and Biskinis 2003; Haselton et al. 2007; Ibarra 2003; Lee and Mosalam 2005). Other researchers studied methods for propagating modeling uncertainties through seismic performance assessments using the first-order second-moment (FOSM) method (Haselton et al. 2007), or a response surface with Monte Carlo simulation (Liel et al. 2009).

State-of-the-art methods for seismic assessment have well-established methods for incorporating RTR variability. However, treatment of modeling uncertainty remains challenging. The term “modeling uncertainty”, as used here, reflects the uncertainty in the extent to which model represents the true structural response. This study evaluates the effect of modeling uncertainty using submissions to a blind prediction contest. In the recent years, different types of structures have been tested on shake tables for the purpose of evaluating seismic design criteria, investigating structural failure modes, or predicting structural response parameters. In some cases, before performing the experiment, teams are invited to predict the response of the structure in so-called “blind predictions”. Participants may predict the response using a variety of modeling techniques and analysis platforms, employing information from design drawings and material properties. The data submitted by participants provide a unique opportunity to study the uncertainty in the predicted response due to modeling.

This study quantifies the significance of modeling uncertainties in seismic performance assessment, using results of a blind prediction contest for a 7-story RC building at UCSD in 2006. These modeling uncertainties reflect differences in software platform, solution algorithm, element type, and model parameter calculation or selection. The effect of some of these sources of uncertainties has not been investigated previously, due to the fact that in most of the past studies, the nonlinear model is simulated using a single software package. After quantifying the modeling uncertainty, this source of uncertainty is combined with the RTR variability in order to investigate the total uncertainty in the results.

## **METHODOLOGY OF STUDY**

This study employs the methodology for assessing the seismic performance of a building developed by the Pacific Earthquake Engineering Research Center, which provides a probabilistic framework for relating ground motion intensity to structural response and performance, through nonlinear time-history simulation (Deierlein 2004). Incremental Dynamic Analysis (IDA) is used to assess global performance as a function of ground motion intensity (Vamvatsikos and Cornell 2002). IDA results show the relationship between ground motion intensity and building response parameters, such as the peak interstory drift ratio, in the structure. The final outcome

of IDA is a set of fragility functions, which define the probability of exceeding a particular drift level or damage state, as a function of the ground motion intensity.

A key challenge in IDA is that the fragility curves so-developed reflect only one source of uncertainty, that coming from randomness of the selected ground motion records, and do not incorporate the uncertainty in the prediction of the drift level which is embedded in the modeling process. This limitation is significant because an analyst usually has only a single model of the structure of interest.

The proposed methodology used to quantify and incorporate modeling uncertainties in the analysis proceeds as follows. First, IDA is performed on a nonlinear model of the case study building for a set of earthquake records, and a set of IDA curves generated, as illustrated in Figure 1a. These IDA curves consider only the randomness due to the earthquake records and are called “IDA-RTR” curves. Modeling uncertainty is then quantified by the variability in results predicted by the participants in the blind prediction contest. Specifically, model predictions of building response submitted by blind test participants are used to quantify histograms of modeled interstory drifts for a particular spectral acceleration level. These histograms are used to fit probability distributions associated with modeling uncertainty.

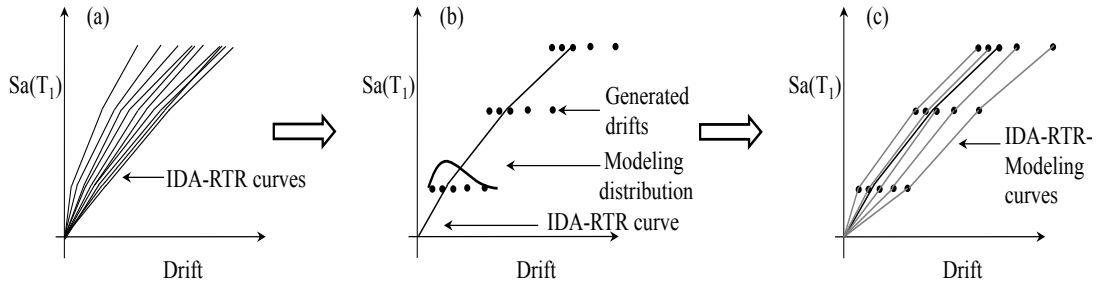


**Figure 1. Schematic drawing illustrating the proposed methodology to consider (a) RTR uncertainty; (b) modeling uncertainty representing the blind prediction test data; and (c) IDA curves generated to represent the modeling uncertainty**

In the next step, modeling and RTR uncertainties are combined. For this purpose, each point on the IDA-RTR curve is replaced by a set of randomly generated points with the same spectral acceleration as the original curve, but a distribution of drifts representing modeling uncertainty. The drifts are generated such that they are probabilistically consistent with the distributions generated in the previous step, as shown in Figure 1b; the distribution used to generate the modeling drifts depends on the drift level. The generated random numbers at different excitation levels are then connected to generate a set of “IDA-RTR-Modeling” curves, as shown in Figure 1c. This set of IDA curves represents the effect of modeling uncertainty, for a given IDA-RTR curve. This process is repeated for all IDA-RTR curves, to generate a new set of IDA curves, known as “IDA-RTR-Modeling”, which incorporate the modeling uncertainty in addition to the RTR variability. This new set of IDA curves is used to compute the fragility curves associated with exceeding particular drift ratios of interest and the results are compared with those from the IDA-RTR curves.

## APPLICATION OF THE PROPOSED METHODOLOGY

**Case study building.** This paper examines the blind predictions submitted for a full-scale 7-story RC wall building tested on the UCSD shaking table, shown in Figure 2. The tested structure represents a slice of a 7-story load bearing wall building typical of Los Angeles construction. The building slice has a reinforced concrete “web” wall, which is the lateral force resisting system, with two transverse “flange” walls, and a post tensioned (PT) segmental precast pier, which provides torsional stability. The floor system is a flat slab supported with steel gravity columns (Panagiotou and Restrepo, 2011). The building was designed based on a displacement-based method, which led to smaller member sizes and less reinforcement than what is required by force-based approach (Panagiotou and Restrepo 2011). The test was conducted to investigate the dynamic response of the building, including the interaction between wall, slab, and gravity system of the building (Panagiotou et al. 2011).



**Figure 2. View of the building tested at UCSD (Moaveni et al. 2011)**

In the experiment, four earthquake records were imposed on the building: 1) the longitudinal component of the 1971 San Fernando earthquake recorded at Van Nuys (EQ.1), which has  $S_a(T_1)$  of 0.32g, 2) the transverse component of the same Van Nuys record, which has  $S_a(T_1)$  of 0.75g, 3) the longitudinal component of the 1994 Northridge earthquake recorded at the Oxnard Boulevard station (EQ.3), which has  $S_a(T_1)$  of 0.60g, and 4) the 360° component of the 1994 Northridge earthquake recorded at the Sylmar station (EQ.4), which has  $S_a(T_1)$  of 1.38g (Moaveni et al. 2011).

**Nonlinear analysis of building.** In order to assess the building's seismic performance in this paper, the nonlinear 2D model of the building developed by Martinelli and Filippou (2009), is analyzed under a set of earthquake records. In this model, the shear wall is simulated with distributed inelasticity force-based beam-columns (Spacone et al. 1996). The cross section is discretized in fibers that capture the interaction of the axial force and bending moment. The compressive behavior of concrete fibers is modeled with the modified Kent-Park material model (Kent and Park 1971); tensile behavior is modeled with a bilinear behavior with a linear elastic branch followed by a linear softening branch. The volumetric confinement effect is

taken into account by the modified Kent-Park model. The nonlinear Menegotto-Pinto material model, modified by Filippou et al. (1983) to include isotropic hardening effects, is used for steel fibers. Each story is modeled with a nonlinear beam-column element with three integration points representing each of the web and flange walls. The post tensioned pier is modeled with linear elastic beam-columns. The connection between the flange and web wall are modeled with rigid end offsets. The mass is lumped at each floor. The footing under each wall is modeled with an elastic element. The period of the model is equal to  $0.49s$ , very close to the experimental fundamental period of  $0.52s$ . The ability of the model to predict the measured earthquake response of the 7-story RC shear wall specimen was demonstrated by the good agreement of the blind prediction results with the measured data, but it did not capture the lap-splice failure observed in the experiment (Martinelli and Filippou, 2009).

The model is analyzed using IDA to develop a fragility curve that accounts for the record-to-record variability. In IDA, the nonlinear structural model is subjected to a recorded ground motion, and dynamically analyzed to predict the structure's response. The time-history analysis is repeated, each time increasing the scale factor on the input ground motion. This process is repeated for a large set of ground motion records. This study uses 35 of the 44 ground motions in the FEMA P-695 far-field set (FEMA 2009). Nine of the 44 ground motions are recognized as the pulse-like ground motions excluded from this analysis (Champion and Liel 2012). The IDA results of the nonlinear model for the selected ground motions are presented in Figure 4a. The use of the FEMA P-695 ground motion set is for illustration only; any set of ground motions selected according to established procedures could be used.

**Description of data.** The data set from the blind prediction test includes structural response predictions for the 7 story building submitted by 21 participant groups for 4 different ground motion time histories. Participants in the blind prediction competition were categorized in three groups: Engineering Practitioners (EP), Undergraduate Students (U), and Researcher Associates (RA). For each ground motion, participants predicted different response parameters of the building, such as maximum moment, maximum interstory drift ratio, maximum shear force, and maximum acceleration at each floor or story. A number of different software platforms were used by the participants including: Abaqus, OpenSees, SAP 2000, Adina, Ram Perform 3-D, and ETABS. The goal of this study is to quantify the modeling uncertainty in the blind prediction data and to assess its influence on the prediction of the ground motion intensity at which a structure experiences drift levels greater than a specified value. As a result, in this study, we focus on the uncertainty in model predictions of maximum interstory drift ratio, which are predicted for each story of the building for each time history. Interstory drift ratio is a dimensionless quantity computed as the difference in lateral deflection between floor  $i$  and floor  $i + 1$ , divided by the height of the story. Aleatory uncertainty associated with material properties is assumed to be reduced because modelers were provided with measured material properties.

Table 1 reports the  $IDR$  values predicted by the practitioner groups for the first earthquake, *i.e.* EQ.1, as an example. The notation  $IDR_{ij}$  in this table refers to the interstory drift ratio for the  $i^{th}$  earthquake record at the  $j^{th}$  story. Table 1 also reports the median and standard deviation of data submitted by all participants for EQ.1, and

the experimentally measured drift ratio. Five out of 21 participant groups are considered to be outliers and dropped from the data set. The outliers are selected based on engineering judgment; specifically, groups reporting predictions of the average *IDR* over all stories that is 10 times greater or smaller than the experimental value for any earthquake record were excluded. The outliers so-identified are thought to have a significant error in the modeling processes, biasing the drift distribution associated with modeling uncertainties.

**Table 1. Predicted (modeled) interstory drifts for the 7-story building for EQ.1**

Participant Group	IDR11	IDR12	IDR13	IDR14	IDR15	IDR16	IDR17
EP1	0.003	0.007	0.009	0.011	0.011	0.012	0.012
EP3	0.001	0.002	0.003	0.003	0.003	0.003	0.003
EP4	0.002	0.004	0.005	0.006	0.006	0.006	0.006
EP5	0.002	0.002	0.002	0.002	0.002	0.002	0.002
EP6	0.003	0.003	0.003	0.003	0.002	0.002	0.001
EP7	0.002	0.003	0.003	0.003	0.003	0.003	0.004
EP8	0.001	0.002	0.003	0.004	0.004	0.004	0.004
Median of all groups	0.002	0.003	0.003	0.003	0.003	0.003	0.004
Standard deviation	0.001	0.002	0.002	0.003	0.003	0.003	0.004
Experimental results	0.001	0.002	0.003	0.003	0.003	0.003	0.003

**Probability distributions of modeled IDR.** Uncertainty in the prediction of *IDR* is not expected to follow the same distribution at all drift ratios because of the increasing complexity with modeling larger drifts reflecting greater nonlinearity in the structure. However, for a given drift level, we expect the distribution of modeled drifts to be similar, regardless of the story or earthquake record for which the drift was modeled and measured. To study the distribution of *IDR* obtained from blind predictions, 6 drift levels measured in the experiment corresponding to  $\Delta_{exp} = 0.003$ , 0.006, 0.009, 0.015, 0.018, and 0.022 are selected. (These values are rounded to the third decimal place.) Each experimental value is compared to the modeled drifts intended to predict that particular experimental value. In some cases this means that model predictions for different stories or earthquake records are combined, provided that all model values were intended to predict the same value of experimental drift,  $\Delta_{exp}$ . The experimental drift levels are selected based on two criteria: 1) for each value of drift, there are a significant number of corresponding modeling predictions reported by participants, and 2) there is enough separation between the selected drift ratios to consider the trend of variation in the modeling drift distribution with increasing *IDR*. Model predictions not corresponding to an experimental drift value in the list above were dropped from the data set. In total, more than 65% of the available data submitted by participants for the displacement field are used in this study. (The authors found that including the omitted in the analysis does not significantly change the findings.)

All modeled drift ratios corresponding to a particular experimental drift  $\Delta_{exp}$  are grouped together. For each drift level, two distributions are fitted. The first distribution is chosen as the best-fit distribution, using the Kolmogorov–Smirnov (K-S) test to measure goodness-of-fit (Massey 1951). Since the best-fit distribution may not be well known, a second distribution which satisfies the K-S test with the 95% confidence level, but is more commonly used (e.g. normal, lognormal, etc.) is also fitted. This second distribution is termed the “engineering fitted” distribution. Figure 3 illustrates the histograms and engineering fitted distributions for two levels of  $\Delta_{exp}$  and the parameters defining these distributions for each drift level are reported in Table 2. The results suggest that the data grouped for  $\Delta_{exp}$  values of 0.015 and 0.018 follow a uniform distribution. This may be due to the limited number of data points at these drift ratios so data corresponding to these two drift levels are not considered in the subsequent analysis.

The data presented in Table 1, and similar model predictions made for the other earthquake records, show a difference or “bias” between the median of the modeling data and the measured value in the experiment. Table 2 reports the bias for each group of data, computed as the difference between the median of modeled value and the experimental value (Montgomery and Runger 2010). This table shows that the models tend to under-predict drifts in comparison to the experiment. Table 2 also shows that the bias increases for larger experimental drifts, which correspond to higher levels of excitation. To study the distribution of drifts associated with modeling uncertainty, two cases are considered. In the first case, the “original” [uncorrected] data, as presented in Table 1, have been used to define the modeling *IDR* distribution directly. In the second case, the bias of data is removed by making the median of the modeling distribution the same as the experimental values, but the dispersion in the modeled data is preserved. This new set of data is called the “unbiased” [corrected] data set.

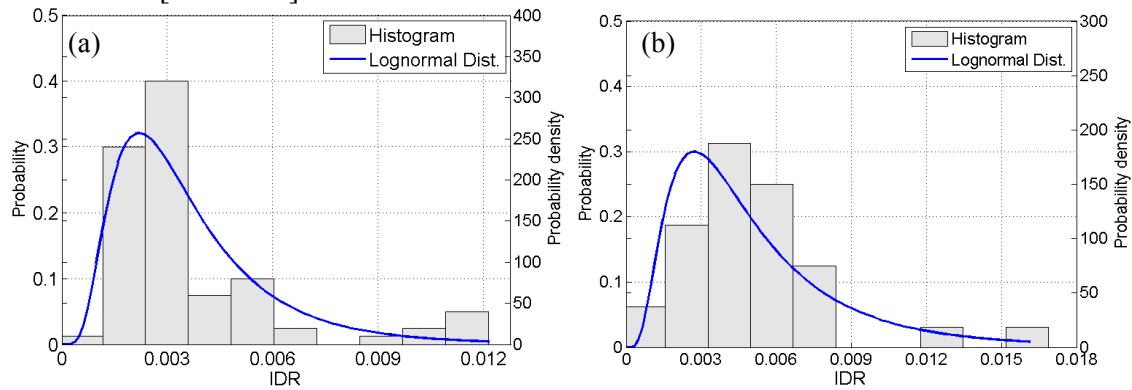


**Figure 3. Histograms and engineering distributions for the “original” prediction data corresponding to (a)  $\Delta_{exp}=0.003$  and (b)  $\Delta_{exp}=0.006$ .**

**Table 2. Statistics of the predicted (modeled) drifts for different experimental drift values**

$\Delta_{exp}$	Best Fit Distribution	Engineering Fit Distribution	Median of Modeled <i>IDR</i>	$\sigma$ of Modeled <i>IDR</i> *	# of Modeled <i>IDR</i> data	Bias
0.003	Burr	Lognormal	0.003	0.003	80	-0.0002

0.006	Cauchy	Lognormal	0.005	0.003	32	-0.0017
0.009	Cauchy	Lognormal	0.007	0.004	95	-0.0022
0.015**	Gen. Pareto	Uniform	0.009	0.005	16	-0.0053
0.018**	Error	Uniform	0.012	0.007	16	-0.0062
0.022	Error	Lognormal	0.016	0.007	64	-0.0055

\* $\sigma$  is the standard deviation of the sample data \*\* Not considered in later analyses

**Combination of modeling uncertainty with RTR uncertainty.** In this section, the modeling uncertainty quantified in the previous section is combined with the RTR uncertainty using the approach described above. The modeling uncertainty is represented by histograms or engineering fitted distributions of the modeled drift values. The effect of modeling uncertainty will be separately considered for the “original” and “unbiased” data sets, for a total of four distinct cases: 1) histograms of the original data; 2) engineering distributions of the original data; 3) histograms of the unbiased data; and 4) engineering distributions of the unbiased data.

**Histograms with the original data.** First, modeling uncertainty is quantified in the form of four histograms corresponding to the  $\Delta_{exp} = 0.003, 0.006, 0.009, 0.022$  and based on the original data. These histograms represent the modeling uncertainty associated with the prediction of a particular drift; each histogram is assumed to be valid for a specified range of drifts. For instance, the histograms corresponding to  $\Delta_{exp} = 0.003$ , is taken to represent the uncertainty in modeling drifts for drifts between zero and 0.0055. Similarly, the histograms corresponding to  $\Delta_{exp} = 0.006, 0.009$ , and 0.022 are taken as the drift distribution for modeled drifts in the ranges of  $0.0055 < \Delta \leq 0.0085$ ,  $0.0085 < \Delta \leq 0.0155$ , and  $0.0155 < \Delta$ , respectively. Modeling uncertainty data are available up to a drift ratio of 0.022. The modeling drift distribution corresponding to  $\Delta_{exp} = 0.022$  is used for all drifts greater than 0.022.

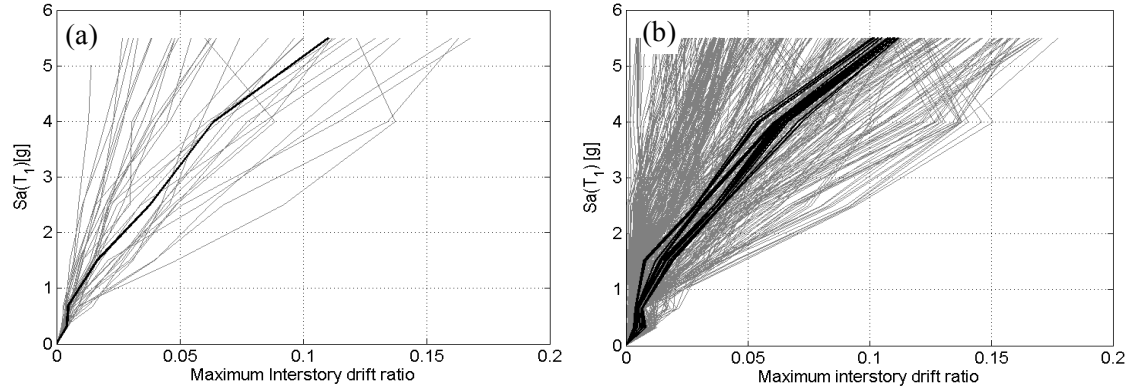
For each IDA-RTR curve, the modeling uncertainty histograms are used to develop IDA-RTR-Modeling curves. These new IDA curves are generated using a Monte Carlo approach, such that for a given excitation level on the IDA-RTR curve, fifty alternative drifts that are consistent with the histogram for the modeled data are simulated.<sup>1</sup> For illustration purposes, ten IDA-RTR-Modeling curves generated for one IDA-RTR curve are shown in black in Figure 4b. This process is repeated for all of the IDA-RTR curves.

To evaluate the effect of propagating the modeling uncertainty through the analysis, a set of fragility curves are computed at different drift levels separately for the IDA-RTR results and IDA-RTR-Modeling results and compared in Figure 5. These fragility curves represent the probability of exceeding a particular drift level, given a specified ground motion intensity. Fragility curves are developed first by computing the empirical CDF of exceeding drift from IDA results and then fitting a lognormal distribution to the data using the maximum likelihood method. Figure 5 also reports the median and lognormal standard deviation of the lognormal fragility curves.

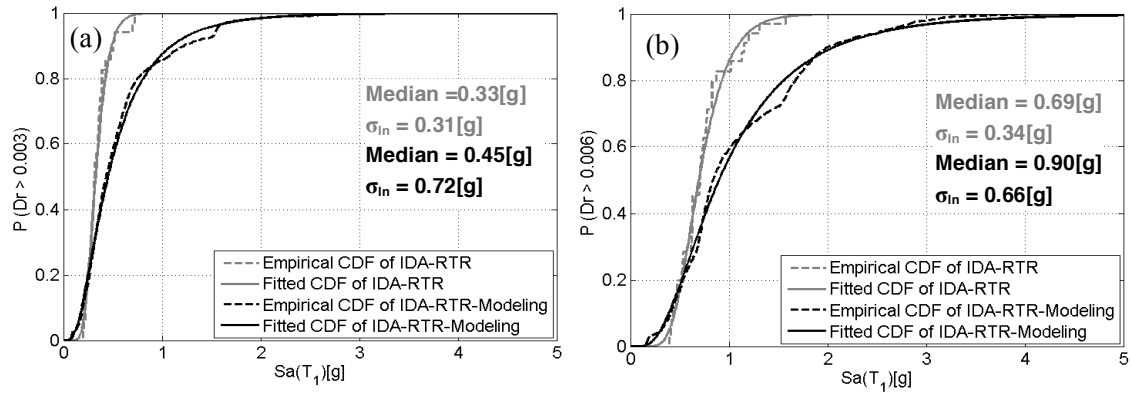
---

<sup>1</sup> Since the histograms shown are for a single value of  $\Delta_{exp}$ , they are shifted if the IDA-RTR has a different value of  $\Delta_{exp}$ .

The incorporation of modeling uncertainty flattens the fragility curve (increasing the dispersion or standard deviation) and increases the median  $S_a$  value. The shift in the median indicates that not incorporating modeling uncertainty can be conservative at high excitation levels, *i.e.* for large  $S_a$  values. This conservatism occurs because the modeled drifts underestimate the true (experimental) drifts. The underestimation is likely due to the use of models that do not reflect the all sources of nonlinearity of the building. The results may also indicate that neglecting modeling uncertainty can be non-conservative at low excitation levels. This could be because of the lack of blind prediction data for drift ratios less than 0.003. Figure 5d shows that the significance of including the modeling variability decreases at the largest drift level (*i.e.* 0.02) and the relative difference between the dispersion of IDA-RTR and IDA-RTR-Modeling is smaller than at the other drift levels. This reduction of dispersion is observed because many of the IDA curves do not have data at this large of a drift. As shown in Table 2, the general trend is that the larger the drift, the greater the dispersion in modeled drift values, which increases the dispersion in the fragility curves. Due to the limited prediction data available at lower drift levels and difficulties in computing fragilities at higher drifts where IDA data are not available, we conclude that the fragility curves computed at drifts of 0.006 and 0.009 are the most representative of the effect of incorporating modeling uncertainty in the seismic assessment results.



**Figure 4. IDA results from nonlinear simulation of the 7-story building, representing: (a) RTR uncertainty, and (b) RTR and modeling uncertainty**



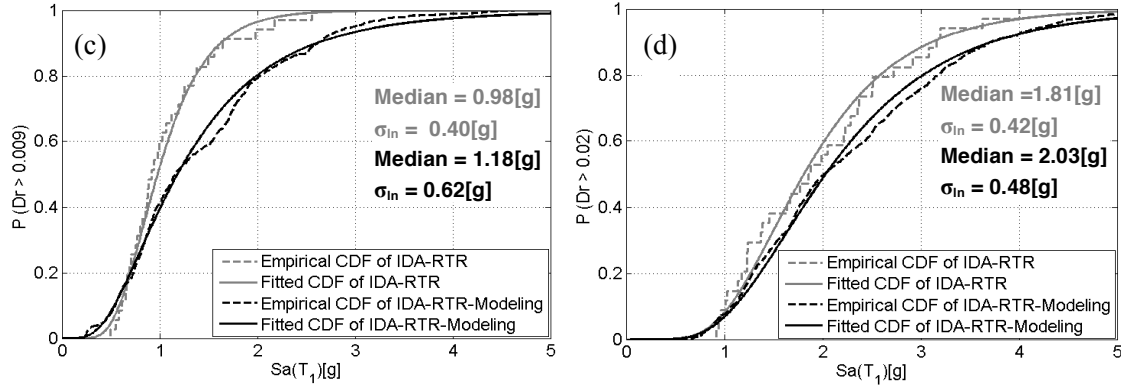


**Figure 5. Comparison between fragility curves computed considering RTR variability only (gray lines) and RTR and modeling variability (black lines) for the original data. The fragility curves computed represent the probability of drifts exceeding a) 0.003, b) 0.006, c) 0.009, and d) 0.02.**

**Histograms with the unbiased data.** In this section, the same procedure is repeated for the unbiased (corrected) data and the results are illustrated in Figure 6. This figure shows that removing the bias from the data virtually eliminates the shift in the median. However, the modeling fragility curve still has larger dispersion than the RTR-only curve because of the uncertainty in the drift prediction, even though on average, the modeled results give the true value.

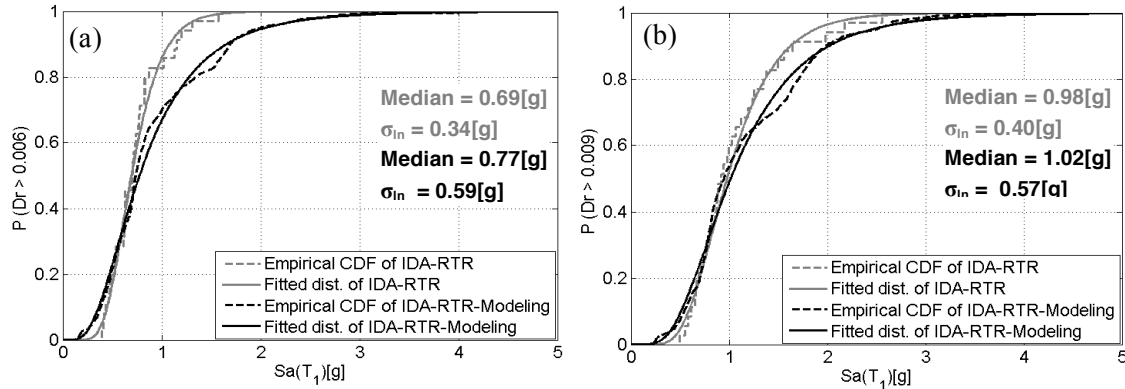


**Figure 6. Comparison between fragility curves computed considering RTR variability only (gray lines) and RTR and modeling variability (black lines) for the unbiased data. The fragility curves computed represent the probability of drifts exceeding a) 0.006 and b) 0.009.**

**Fitted distributions with the original data and unbiased data.** In this section, the same procedure, as explained in the previous two sections, is repeated, except that the randomly generated model drifts are simulated using the engineering distributions, instead of the histograms. The process is repeated for the original and unbiased data, and the median and standard deviation of the fitted fragility curves are presented in Table 3. For comparison purposes, the median and standard deviation of the previous results (Figures 5 and 6) are also summarized in Table 3. Comparison of the results shows that the distribution and histograms lead to very similar medians and standard deviation of the developed fragility curves. This finding implies that either of these two approaches can be implemented to incorporate the modeling

uncertainty in seismic assessment process. However, using the engineering distribution is likely to be more straightforward in practice.

**Table 3. Median and standard deviation of the fragility curves representing uncertainty in RTR and modeling, obtained from histogram and distribution approaches**

Drift	Histograms & Original data		Histograms & Unbiased data		Distributions & Original data		Distributions & Unbiased data	
	Median Sa(T <sub>1</sub> ) [g]	$\sigma_{ln}$ [g]	Median Sa(T <sub>1</sub> ) [g]	$\sigma_{ln}$ [g]	Median Sa(T <sub>1</sub> ) [g]	$\sigma_{ln}$ [g]	Median Sa(T <sub>1</sub> ) [g]	$\sigma_{ln}$ [g]
0.006	0.90	0.66	0.77	0.59	0.88	0.69	0.73	0.61
0.009	1.18	0.62	1.02	0.57	1.21	0.61	1.02	0.51

## CONCLUSION AND RECOMMENDATIONS

This study quantifies the effect of modeling uncertainty on seismic fragility assessments, using results of the 7-story RC building blind prediction contest at UCSD. The modeling uncertainty is presented in terms of drift distributions based on the modeled drift submitted by the contest participants. These distributions are evaluated at different drift levels measured during the experiment. The modeling drift distributions are propagated through the results of the nonlinear time history analyses that consider only the record-to-record (RTR) variability. The resulting IDA curves are used to compute the fragility curves to represent the probability of exceeding a particular drift level as a function of ground motion intensity. The results showed that incorporating the modeling uncertainty to the RTR variability results leads to an increase in the median Sa level and increase the dispersion of the fragility curve by the average of 25% and 73%, respectively. The predicted increase in the dispersion is greater than that obtained by other methods for quantifying modeling uncertainty (e.g. Haselton et al. 2007). Analyses results showed that the main portion of the shift in the median is due to the bias existing in the modeled data for this test.

This study developed and tested the proposed methodology to incorporate the modeling uncertainty to the seismic assessment procedure based on blind prediction test data. The blind prediction test data represents a unique opportunity to quantify modeling uncertainties. The results of this study suggest that modeling uncertainties can be incorporated by introducing a drift distribution to represent the modeling uncertainty. However, the main challenge is understanding the modeling drift distributions, which involves more research to predict generalizable modeling drift distribution applicable to a wider range of buildings. The numbers and distributions presented in this paper are valid only for this case study building. A remaining question is whether the level of underprediction in the contest submissions is typical.

## ACKNOWLEDGMENTS

The authors would like to thank Prof. Marios Panagiotou from UC Berkeley and Prof. Jose Restrepo from UC San Diego for sharing the blind prediction data.

## REFERENCES

- Champion, C., and Liel, A. (2012). "The effect of near-fault directivity on building seismic collapse risk." *Earthquake Engineering & Structural Dynamics*, 41(10), 1391–1409.
- Deierlein, G. G. (2004). "Overview of a comprehensive framework for earthquake performance assessment." *Overview of a comprehensive framework for earthquake performance assessment, PEER Rep. 2004/05*, Berkeley, 15–26.
- Ellingwood, B., Galambos, T. V., MacGregor, J. G., and Cornell, C.A. (1980). *Development of a Probability-Based Load Criterion for American National Standard A58*. National Bureau of Standards, Washington.
- Fardis, M. N., and Biskinis, D. E. (2003). "Deformation capacity of RC members, as controlled by flexure or shear." *Otani Symposium*, 511–530.
- FEMA. (2009). *Quantification of Building Seismic Performance Factors (FEMA P695)*. Applied Technology Council, Redwood City, CA.
- Filippou, F. C., Popov, E. P., and Bertero, V. V. (1983). "Effects of bond deterioration on hysteretic behavior of reinforced concrete joints."
- Haselton, Curt B., Goulet, C. A., Mitrani-Reiser, J., Beck, J. L., Deierlein, Gregory G., and Porter, K. A. (2007). *An Assessment to Benchmark the Seismic Performance of a Code-Conforming RC Moment-Frame Building*.
- Ibarra, L. (2003). "Global Collapse of Frame Structures Under Seismic Excitations." Ph.D., Stanford University.
- Kent, D. C., and Park, R. (1971). "Flexural Members with Confined Concrete." *Journal of the Structural Division*, 97(7), 1969–1990.
- Lee, T.-H., and Mosalam, K. M. (2005). "Seismic demand sensitivity of reinforced concrete shear-wall building using FOSM method." *Earthquake Engineering & Structural Dynamics*, 34(14), 1719–1736.
- Liel, A. B., Haselton, C. B., Deierlein, G. G., and Baker, J. W. (2009). "Incorporating modeling uncertainties in the assessment of seismic collapse risk of buildings." *Structural Safety*, 31(2), 197–211.
- Moaveni, B., He, X., Conte, J. P., Restrepo, J. I., and Panagiotou, M. (2011). "System Identification Study of a 7-Story Full-Scale Building Slice Tested on the UCSD-NEES Shake Table." *Journal of Struc. Engineering*, 137(6), 705–717.
- Montgomery, D. C., and Runger, G. C. (2010). *Applied Statistics and Probability for Engineers*. Wiley.
- Panagiotou, M., and Restrepo, J. I. (2011). "Displacement-Based Method of Analysis for Regular Reinforced-Concrete Wall Buildings: Application to a Full-Scale 7-Story Building Slice Tested at UC–San Diego." *Journal of Structural Engineering*, 137(6), 677–690.
- Panagiotou, M., Restrepo, J. I., and Conte, J. P. (2011). "Shake-Table Test of a Full-Scale 7-Story Building Slice. Phase I: Rectangular Wall." *Journal of Structural Engineering*, 137(6), 691–704.
- Spacone, E., Filippou, F. C., and Taucer, F. F. (1996). "Fibre Beam–Column Model for Non-Linear Analysis of R/C Frames: Part I. Formulation." *Earthquake Engineering & Structural Dynamics*, 25(7), 711–725.
- Vamvatsikos, D., and Cornell, C. Allin. (2002). "Incremental dynamic analysis." *Earthquake Engineering & Structural Dynamics*, 31(3), 491–514.